28PG1 APPLICATION OF DECONVOLUTION TECHNIQUES TO LIDAR SIGNALS

D. Peri, S. Egert, J. Sivan
Israel Institute for Biological Research
P.O. Box 19, Ness-Ziona, Israel 70450

INTRODUCTION

LIDAR systems, based on a CO_2 pulsed laser, are limited in their range resolution by the laser pulse duration. The laser pulse duration is mainly determined by a phenomenon known as the "nitrogen tail", a result of an inefficient transfer of energy from the nitrogen molecules to the CO_2 molecules. The laser pulse starts with a narrow spike of 100-200nS duration, followed by a slow decay ("tail") of a few microseconds, which contains more than half of the pulse energy. When the detection process is linearly scaled, as opposed to some systems that are logarithmicly scaled, the resulting signal is a convolution of an ideal signal with the transmitted pulse signal. The convolution process acts as a low-pass filter that suppresses details shorter than the pulse duration. Since the transmitted pulse is readily monitored, a process of deconvolution is possible.

Some factors involved in the deconvolution process should be handled with care. A proper estimation of the noise power spectral density must be performed. This can be done either by analyzing digitized samples of detected signals or by applying theoretical models, as for example, in the case of quantization noise. Consideration should be also given to the averaging procedure involved in the detection process. The averaging deals with two other processes that have stochastic character: Variable pulse shape and variable pollutant concentration in the measured field.

Additional difficulties arise due to the logarithmic transformation applied in the process of concentration calculations. The deconvolution process involves some kind of high-pass filtering. Typical to such filtering is the appearance of spurious oscillations near abrupt changes, and a reduction of the DC component in the Fourier transform representation. Both phenomena likely to cause the reconstructed signal to have regions of negative values. The logarithmic transformation cannot handle non-positive values.

In the analysis of experimental data, we have encounter an additional problem: The monitored pulse shape seems to be somewhat distorted, resulting in an inaccurate reconstruction of the signal. To deal with this problem, blind deconvolution techniques have been applied.

ANALYSIS METHODS

The signal, s(t), resulting from the convolution process, is mathematically expressed in Eq. 1;

$$s(t) = \int g(u)h(t-u)du + n(t) \equiv g*h + n \qquad (1)$$

where g(t) is the signal to be reconstructed, h(t) is the laser pulse shape function, normalized to have unit area, and n(t) is an additive, zero mean, noise term. The asterisk represents the convolution integral operation. Direct inverse filtering performs poorly since the filter design ignores the noise process. Improved restoration quality is possible with Wiener filtering techniques, which incorporate a priori statistical knowledge of the noise term [1]. The filter function, expressed in the Fourier domain, is given by,

$$F(\tau) = H^*(\tau)/[|H(\tau)|^2 + SNR(\tau)^{-1}] \qquad (2)$$

where $SNR(\tau) \equiv \Phi_g(\tau)/\Phi_n(\tau)$ is the signal-to-noise power spectral

density ratio, and upper case functions designate the Fourier transform of the corresponding lower case ones. An estimation of $\Phi_n(\tau)$ is readily derived by averaging the square of absolute value of the Fourier transform of samples of measurements data, $\langle|S(\tau)|^2\rangle$. To estimate $\Phi(\tau)$ at low frequencies, where $G(\tau)H(\tau)$ have significant values, is done by extrapolation of the function from its values at higher frequencies. The estimation of $\Phi(\tau)$ is less straightforward. We start with a crude estimate, $\Phi_g(\tau)\approx\langle|S(\tau)|^2\rangle-\Phi_n(\tau)$. At the first iteration $G(\tau)$ is calculated from $F(\tau)\cdot S(\tau)$. This result is used for an improved estimation, $\Phi_g(\tau)\approx|G(\tau)|^2$. In principle this process can be extended to more iterations, however it is not necessary, because the filter function is not very sensitive to the exact functional behavior of SNR^{-1}. It mainly depends on the frequency region where the SNR changes from being much larger to much smaller than $|H(\tau)|^2$.

An application of Wiener filtering does not always result in a reasonable accuracy of signal reconstruction. It works well for cases where the concentration path integral (CL) is in a limited range of values and also the field width is not excessively large. High gas concentration cause an abrupt cut of the returned signal which results in the appearance of spurious oscillations. Zero crossings and regions of negative values prevent the extraction of concentration information, since the process involves a logarithmic transformation. Further considerations led us to conclude that the monitored transmitted pulse shape does not represent accurately the real laser power. A situation where the system impulse response is not fully known calls for an application of blind deconvolution (BD) techniques [2,3]. Iterative algorithms developed for BD make it possible to impose desired constraints in the time domain while the constraints in the Fourier domain remain the conventional Wiener filter. The time domain constraints can be the non-negativity requirement together with some other constraints that express a priori knowledge about the expected shape of the solution. For example, we can apply constraints that force the solution to be zero at t=0 and rise gradually according to a calculated form of the overlap function.

The Fourier domain constraints used in the k-th iteration are Wiener type filters, expressed by Eqs. (3),

$$G_k = S\cdot H^*_k/[|H_k|^2 + (SNR_{G,k-1})^{-1}] \qquad (3\text{-a})$$

$$H_{k+1} = S\cdot G_k/[|G_k|^2 + (SNR_{H,k})^{-1}]. \qquad (3\text{-b})$$

Figure 1 below illustrates the steps of the iterative algorithm.

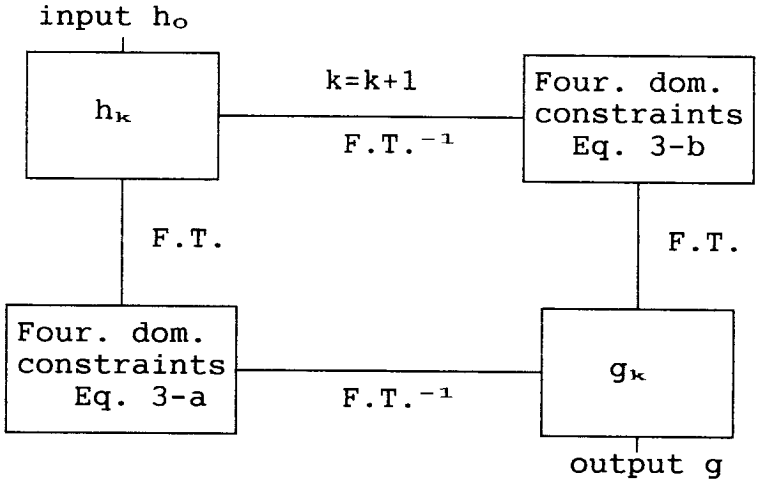

Figure 1: Outline of the iterative algorithm. F.T. designates Fourier-Transformation and F.T.$^{-1}$ inverse transformation.

COMPUTER SIMULATIONS

In the limited scope of this manuscript we present only a few computer simulations. Processing of real data and more computer simulations will be presented at the conference meeting. Figure 2-a shows synthetic signals that represent the returned pulses smeared the convolution process, together with an additive white noise. One signal is attenuated by absorption (on-line) and the other unaffected (off-line). Also shown are the deconvolved signals after two iterations. Figure 2-b depicts the retrieved distribution of pollutant concentration using the iterative Wiener filtering. The first iteration gives a quit noisy result. The second iteration gives a much less noisy distribution which shows a good fit to the original distribution.

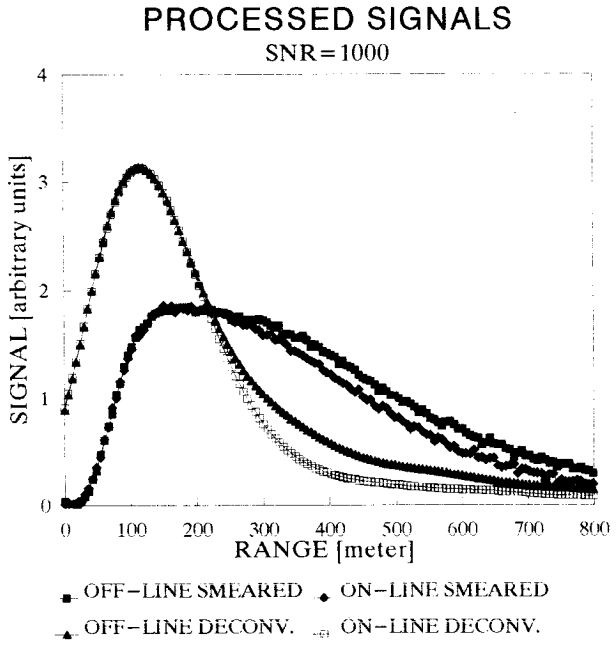

Fig. 2-a

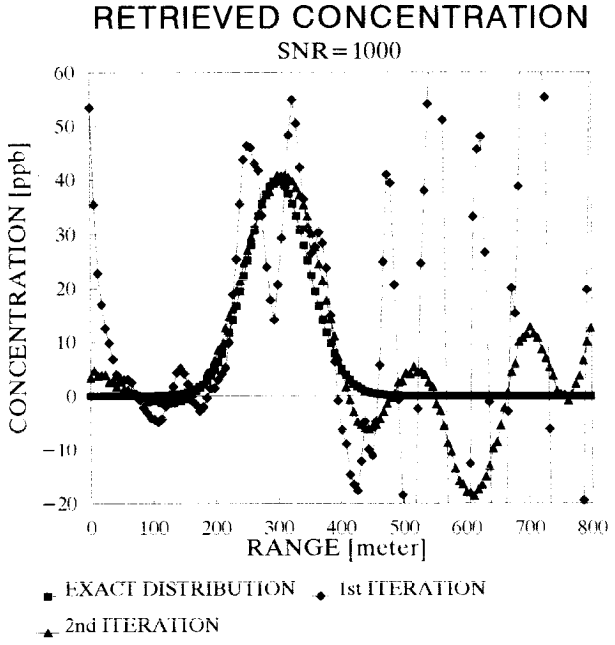

Fig. 2-b

Figure 2: Computer simulations. (a) Smeared and deconvolved signals. (b) Reconstructed pollutant concentration.

REFERENCES

1. C.W. Helstrom, "Image Restoration by the Method of Least Squares", J. Opt. Soc. Am. 57, 293-303, (1967).
2. N. Nakajima, "Blind Deconvolution Using the Maximum Likelihood Estimation and the Iterative Algorithm", Opt. Commun. 100, 59-66, (1993).
3. N. Miura, S. Kuwamura, N. Baba, S. Isobe and M. Noguchi, "Parallel Scheme of the Iterative Blind Deconvolution Method for Stellar Object Reconstruction", Appl. Opt. 32, 6514-6520, (1993).